Electronic Energy Migration on Different Time Scales: Concentration Dependence of the Time-Resolved Anisotropy and Fluorescence Quenching of Lumogen Red in Poly(methyl methacrylate)

Kathryn A. Colby, Jonathan J. Burdett, Robert F. Frisbee, Lingyan Zhu, Robert J. Dillon, and Christopher J. Bardeen*

Department of Chemistry, University of California, Riverside, Riverside, California 92521

Received: October 27, 2009; Revised Manuscript Received: January 23, 2010

Electronic energy transfer plays an important role in many types of organic electronic devices. Förster-type theories of exciton diffusion provide a way to calculate diffusion constants and lengths, but their applicability to amorphous polymer systems must be evaluated. In this paper, the perylenediimide dye Lumogen Red in a poly(methyl methacrylate) host matrix is used to test theories of exciton motion over Lumogen Red concentrations (C_{LR}'s) ranging from 1×10^{-4} to 5×10^{-2} M. Two experimental quantities are measured. First, time-resolved anisotropy decays in films containing only Lumogen Red provide an estimate of the initial energy transfer rate from the photoexcited molecule. Second, the Lumogen Red lifetime decays in mixed systems where the dyes Malachite Green and Rhodamine 700 act as energy acceptors are measured to estimate the diffusive quenching of the exciton. From the anisotropy measurements, it is found that theory accurately predicts both the C_{LR}^{-2} concentration dependence of the polarization decay time τ_{pol}, as well as its magnitude to within 30%. The theory also predicts that the diffusive quenching rate is proportional to C_{LR}^{α}, where α ranges between 1.00 and 1.33. Experimentally, it is found that $\alpha = 1.1 \pm 0.2$ when Malachite Green is used as an acceptor, and $\alpha = 1.2 \pm 0.2$ when Rhodamine 700 is the acceptor. On the basis of the theory that correctly describes the anisotropy data, the exciton diffusion constant is projected to be 4−9 nm^2/ns. By use of several different analysis methods for the quenching data, the experimental diffusion constant is found to be in the range of 0.32−1.20 nm^2/ns. Thus the theory successfully describes the early time anisotropy data but fails to quantitatively describe the quenching experiments which are sensitive to motion on longer time scales. The data are consistent with the idea that orientational and energetic disorder leads to a time-dependent exciton migration rate, suggesting that simple diffusion models cannot accurately describe exciton motion within this system.

Introduction

Electronic energy transfer (EET) plays an important role in the function of many devices based on conjugated organic materials. In organic light-emitting diodes, exciton diffusion can decrease device efficiency through enhanced luminescence quenching at defect sites.[1] In organic photovoltaics, on the other hand, rapid exciton diffusion is beneficial, since it increases the probability that the exciton will reach an interface and undergo charge separation to generate photocurrent.[2,3] Fluorescent sensors based on conjugated polymers often rely on exciton migration to amplify the effect of an analyte binding event.[4] Given the current interest in organic materials for optoelectronic applications, it is desirable to have a tractable model that can predict quantities like the exciton diffusion length. In highly ordered systems with strong electronic coupling, like molecular crystals, such models are difficult to formulate because the aggregate electronic states, such as delocalized Frenkel and charge-transfer excitons, are still not completely understood. In such systems, the role of electronic coherence and delocalization in the EET dynamics remains an area of active investigation.[5−10] However, when the excited state is localized on a single molecular site, and EET proceeds by incoherent hopping, the dynamics can be described in terms of a simple rate process given by Förster resonance energy transfer (FRET) theory. The FRET rate (k_{FRET}) between any two sites separated by a distance R is given by the Förster rate equation[11]

$$k_{FRET} = \frac{1}{\tau_{FRET}} = \frac{1}{\tau_{fl}}\left(\frac{R_0}{R}\right)^6 \tag{1a}$$

$$R_0^{\,6} = \frac{9000 \ln(10)\phi_{fl}\kappa^2}{128\pi^5 N_A n^4}\int_0^\infty \varepsilon(\nu) f(\nu)\frac{d\nu}{\nu^4} \tag{1b}$$

where R is the separation between chromophores, n is the index of refraction, τ_{fl} is the fluorescence lifetime of the donor, ϕ_{fl} is the fluorescence quantum yield, κ is an orientation factor, N_A is Avagodro's number, $\varepsilon(\nu)$ is the absorption spectrum of the acceptor, and $f(\nu)$ is the donor's fluorescence spectrum whose integral has been normalized to 1. R_0 combines these factors into a single length called the critical Förster radius, the distance for which there is a 50% probability for electronic energy transfer to occur relative to other deactivation pathways. When multiple EET events occur between molecules of the same type, the phenomenon is termed energy migration or exciton diffusion.

* To whom correspondence should be addressed, christopher.bardeen@ucr.edu.

10.1021/jp910277j
Published on Web 02/19/2010

In his original paper,[11] Förster derived a theoretical expression for the exciton diffusion constant D through a three-dimensional lattice in terms of these parameters, which has been rederived by subsequent workers[12−16]

$$D = \eta\left(\frac{4\pi C}{3}\right)^{4/3}\frac{R_0^{\,6}}{\tau_{\mathrm{fl}}} \tag{2}$$

where C is the chromophore number density, the prefactor η ranges between 0.30 and 0.56, and all the constants are as previously defined. Equation 2 leads directly to an equation for the exciton diffusion length L_{D} in the absence of quenchers

$$L_{\mathrm{D}} = \sqrt{6D\tau_{\mathrm{fl}}} = \sqrt{6\eta}\left(\frac{4\pi C}{3}\right)^{2/3}R_0^{\,3} = 6.36\sqrt{\eta}C^{2/3}R_0^{\,3} \tag{3}$$

Equations 2 and 3 provide a straightforward way to predict the diffusion of electronic excitations through a material using easily accessible experimental quantities like the overlap of absorption and fluorescence spectra. An organic dye with a small fluorescence Stokes shift and high quantum yield can easily possess a critical radius $R_0 \sim 5$ nm for self-transfer. If the concentration of such a dye could be raised to $C \sim 1$ molecule/nm,[3] eq 3 predicts that diffusion lengths on the order of 100 nm should be observable. Unfortunately, such long diffusion lengths are almost never observed in conjugated organic materials. There are several reasons why eqs 2 and 3 may break down for real systems. First, the assumption of point dipole−dipole interactions breaks down as the interchromophore separation decreases, necessitating a more realistic model for the chromophore−chromophore interaction which explicitly takes into account molecular shape and size as well as higher multipole interactions. Second, the model assumes that the motion is diffusive at all times, while more sophisticated approaches have shown that positional, energetic, and orientational disorder can all lead to anomalous behavior on different time scales. Finally, many chromophores tend to exhibit concentration-dependent aggregation behavior. Such aggregates can lead to low-energy electronic states, like excimers, that act as trapping sites and interfere with exciton migration. Due to these shortcomings, it is worth asking under what circumstances eqs 2 and 3 possess significant predictive value. Even if the physical reality of molecular size, disorder, etc., makes it impossible to rely on eqs 2 and 3 to predict the absolute values for D and L_{D}, they may still provide a valid way to interpret trends in these quantities as parameters like C, R_0, and τ_{fl} are varied. If the simple diffusion model captures the essential physics of exciton migration through amorphous solids, it can still be a useful tool for the design and optimization of organic electronic materials. On the other hand, it may be that numerical simulations are the only method to provide a reliable picture of energy migration in disordered condensed phase systems.

In this paper, we evaluate the ability of eqs 2 and 3 to describe both the absolute kinetic parameters of intermolecular exciton diffusion and their trends with chromophore concentration. Our test molecule is 1,6,7,12-tethraphenyl ether 2,2′-*N*,*N*′-di(1,3-diisopropylbenzene)-diimide 3,4,9,10-perylenetethracarbon acid, commonly known as Lumogen Red (LR), a perylenediimide dye with good photophysical properties that is also resistant to aggregation. From a practical standpoint, LR has been shown to be extremely photostable relative to other organic dyes, a mandatory requirement for optoelectronic applications. In addition, LR possesses a high extinction coefficient accompanied by a small Stokes shift, both of which allow for optimal EET efficiencies. In this work, we measure the time-resolved luminescence in order to monitor two quantities that are directly related to the exciton diffusion rate. The first quantity of interest is the anisotropy decay, while the second is the fluorescence quenching rate due to energy transfer to an acceptor molecule doped into the donor/polymer host. Both types of experiments have been used extensively to characterize EET in condensed phases but are sensitive to different periods of the exciton evolution. Anisotropy probes the first transfer event away from the initially excited molecule, while fluorescence quenching is sensitive to the total distance covered by the exciton during its lifetime. Taken together, the experiments are designed to test both the quantitative and the qualitative predictions of simple FRET-based theories. Through these experiments, we are able to show that the Gouchanour−Anderson−Fayer (GAF) theory successfully describes how the anisotropy decay rate depends on LR concentration up to 50 mM. In fact, the theory provides an almost quantitative prediction for the anisotropy decay time τ_{pol}. Related theories also predict the observed concentration dependence of the fluorescence quenching rate but overestimate the value of the experimentally derived diffusion constant by roughly a factor of 3−10. Thus the applicability of the simple theory appears to depend on the process being measured. Possible reasons for this discrepancy are discussed, including nonrandom distributions of donors and/or acceptors, deviations from the point-dipole approximation, perturbation of the exciton diffusion by the presence of acceptor molecules, and the possible role of static energetic and orientational disorder that results in anomalous subdiffusion. The results in this paper suggest that theories that rely on a single diffusion constant are insufficient to fully describe exciton migration through amorphous polymer films with and without acceptors. There is clearly a need for more sophisticated theories that can be used to analyze experimental data in a tractable way.

Experimental Section

Sample Preparation. Lumogen Red (LR) was donated by BASF. It was stored in the dark at room temperature and purified by silica gel column chromatography using a 0.9/0.1 by volume chloroform/hexane eluant. Purity was determined to be greater than 98% by LC-MS and ^{1}H NMR. The quenching dyes Malachite Green (MG) and Rhodamine 700 (R700), obtained from Exciton, were used without further purification. The poly(methyl methacrylate) (PMMA) (MW $\approx$ 120000 g/mol, Aldrich), chloroform (Fisher Scientific), and hexanes (Fisher Scientific) were used as received. Thin films for the anisotropy experiments were spin-coated at 300−3000 rpm from chloroform solutions with appropriate PMMA:LR ratios to produce $10^{-4}$to 5×10^{-2} M LR films with peak optical densities $\leq$0.20. These low optical densities are necessary to avoid optical artifacts due to self-absorption and saturation. All the films were optically clear. Film thicknesses for the samples used in the anisotropy experiment were measured on a Veeco DekTak8 profilometer and found to be in the range of 260−4000 nm. The absorption coefficient, ε, of LR in PMMA was measured to be 49900 ± 400 M^{-1} cm^{-1} at the peak absorption, located at 572−575 nm depending on concentration. With these thicknesses and the film absorptions measured on a Cary-Bio50 UV−vis spectrometer, the LR concentrations were confirmed using Beer's law. Films for the variable donor and variable acceptor sensitization experiments were prepared in a similar fashion, with chloroform stock solutions prepared with the

appropriate PMMA:LR:dopant ratios. For the variable donor experiment, films in the range of 10^{-4} to 5×10^{-2} M LR were doped with either 2 mM Rhodamine 700 or 4 mM Malachite Green. For the variable acceptor experiment, 10 mM LR films were doped with $10^{-4}-10^{-2}$ M Rhodamine 700.

Steady-State Measurements. Steady-state absorption spectra were taken on a Cary-Bio50 spectrometer throughout the range of 350−700 nm. Steady-state fluorescence spectra were obtained from a Horiba Jobin Yvon-Spex Fluorolog-3 fluorimeter with front face detection and 500 nm excitation, with spectra collected within the range of 525−750 nm. The fluorescence spectra were independent of excitation wavelength.

Time-Resolved Anisotropy Measurements. Data for the anisotropy experiments were obtained using a Ti−sapphire regeneratively amplified laser system that generates 120 fs pulses, centered at 800 nm, at a 40 kHz repetition rate. The 550 nm excitation beam was produced by continuum generation in a 2 mm thick sapphire plate followed by a 550 nm interference filter with a 10 nm nominal bandwidth. The beam was directed through a polarizer and onto a sample protected from air exposure inside an evacuated cryostat. The polarization of the excitation beam was controlled using a calcite polarizer. Fluorescence from the sample was directed through a thin film polarizer, an OG-570 Schott glass filter, and onto the entrance slit of a Hamamatsu C4334 Streakscope streak camera. Fluorescence decays polarized parallel $I_{\parallel}(t)$ and perpendicular $I_{\perp}(t)$ to the excitation beam were collected by the rotation of the thin film polarizer placed before the entrance slit of the streak camera monochromator. Raw $I_{\parallel}(t)$ and $I_{\perp}(t)$ decays were integrated over the wavelength range 575−700 nm and then smoothed with five-point adjacent averaging. The background noise was subtracted, and the time axes were adjusted via the technique of front-edge matching[17] prior to calculating the anisotropy decays, $r(t)$, using the formula

$$r(t) = \frac{I_{\parallel}(t) - I_{\perp}(t)}{I_{\parallel}(t) + 2I_{\perp}(t)} \tag{4a}$$

The total fluorescence decay, $I(t)$, was determined using the formula

$$I(t) = I_{\parallel}(t) + 2I_{\perp}(t) \tag{4b}$$

The ratio corresponding to the parallel and perpendicular detection sensitivities (sometimes termed the G factor[18]) was previously found to be unity for the experimental setup.

Time-Resolved Sensitization Experiments. The same laser setup was used but with the detection polarizer set to the magic angle 54.7° with respect to the incident beam to negate the effects of rotational diffusion. LR fluorescence in the range from 570 to 620 nm was collected for the case when Rhodamine 700 (R700) was acting as the acceptor and in the range from 570 to 605 nm for the case of Malachite Green (MG). The limited wavelength ranges prevented contributions from the fluorescence of R700 (peak at 669 nm) and MG (peak at 647 nm) from contaminating the donor (LR) fluorescence decay data. Raw data were smoothed with five-point adjacent averaging and the background noise was subtracted prior to dividing two decay curves to extract "A", the energy diffusion term defined in eq 12. Fits were made starting at a delay of 0.2 ns after the initial peak to avoid excess noise in the decay due to scatter from the excitation pulse.

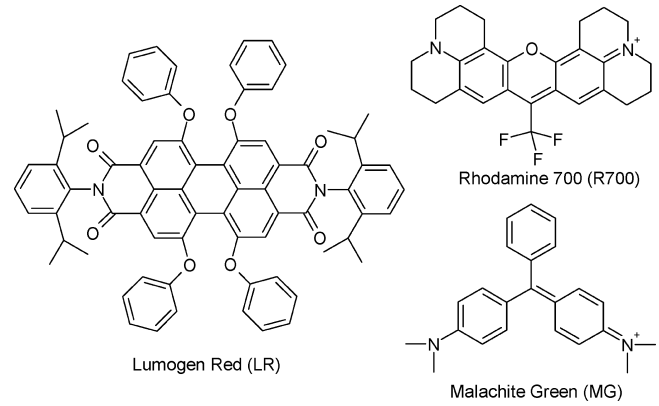

Figure 1. Molecular structures for Lumogen Red, Rhodamine 700, and Malachite Green.

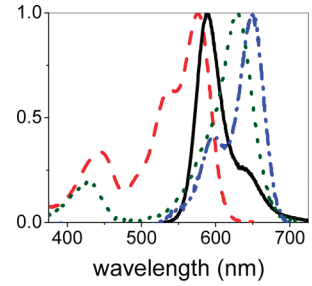

Figure 2. Steady-state absorption and fluorescence spectra used to calculate $R_0^{LR\rightarrow LR}$, $R_0^{LR\rightarrow R700}$, and $R_0^{LR\rightarrow MG}$: Lumogen Red absorption (dashed red line) and fluorescence (solid black line), Rhodamine 700 absorption (blue dot dashed line), and Malachite Green absorption (green dotted line).

Results

Photophysical Properties of Energy Transfer Systems. The chemical structure of our donor molecule, the perylenediimide dye Lumogen Red (LR), is shown in Figure 1 along with the structures of the acceptor molecules Rhodamine 700 (R700) and Malachite Green (MG). The perylenediimide dyes are very stable molecules whose physical properties can be tuned by synthetic methods[19,20] and whose n-type conduction properties make them candidates for inclusion in organic electronic devices like organic photovoltaics.[21−24] LR itself has been investigated for potential applications in luminescent solar concentrators,[25−28] solid-state organic lasers,[29−31] and light-emitting diodes.[32,33] LR is a highly substituted derivative with a fluorescence quantum yield $\tau_{fl} = 0.96$, a relatively long fluorescence lifetime $\tau_{fl} =$ 6.0 ns, and a small Stokes shift (~650 cm^{-1}), all measured in dilute solution.[25] We found previously that LR is also relatively resistant to aggregation-induced fluorescence quenching.[34] Thus, in many respects, LR is an ideal molecule for testing the predictions of exciton diffusion theory. Figure 2 shows the LR fluorescence spectrum along with the LR, R700, and MG absorption spectra in PMMA. It can be seen that the LR emission has reasonably good overlap with all three absorption spectra, leading to Förster critical radii of $R_0^{LR\rightarrow LR} = 5.05$ nm, $R_0^{LR\rightarrow R700} = 5.85$ nm, and $R_0^{LR\rightarrow MG} = 5.93$ nm, where $R_0^{X\rightarrow Y}$ refers to the Förster radius for X to Y energy transfer. These values were calculated using eq 1b for 1 mM LR in PMMA assuming a fluorescent quantum yield of 0.88 and a fluorescence lifetime of 5.7 ns for LR in PMMA, an orientational factor $\kappa^2 = 0.476$ as theorized for a random arrangement of stationary molecules,[35] and a refractive index of 1.49 for PMMA. Note that LR's fluorescence quantum yield and lifetime decrease slightly when the dye is embedded in a polymer host like

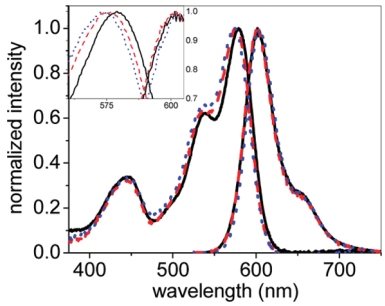

Figure 3. Spectral shifting of Lumogen Red absorption and fluorescence spectra with changing concentration in PMMA. The concentrations are 10^{-4} M (black solid line), 5 mM (red dashed line), and 50 mM (blue dotted line) LR in PMMA. The detailed peak shifts are shown in the inset of the figure.

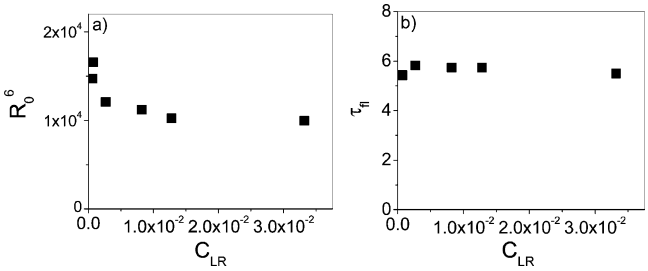

Figure 4. For LR in PMMA concentrations ranging from 1 to 50 mM, (a) R_0^6 decreases due to the spectral shifting shown in Figure 3, but (b) τ_{fl} remains unchanging over this concentration range.

PMMA.[36] The red-shifted fluorescence spectra of R700 (peaked at 669 nm) and MG (peaked at 647 nm) make it possible to isolate the LR donor fluorescence decays from those of the acceptor molecules.

It is well-known that the spectroscopic properties of a molecule can change as its concentration is increased, and this is also the case for LR in PMMA. As the concentration of LR is increased up to 50 mM, the absorption broadens slightly and experiences a blue shift of ~4 nm while the emission undergoes a slight red shift, as shown in Figure 3. These shifts, which can be ascribed to solvatochromic effects arising from the higher density of polarizable electrons in the medium, are sometimes referred to as solid-state solvation.[37] The net effect that these shifts have on energy transfer is to reduce the spectral overlap and thus $R_0^{LR\rightarrow LR}$. The dependence of the calculated values of $R_0^{LR\rightarrow LR}$ on concentration is given in Figure 4a. This figure shows that $R_0^{LR\rightarrow LR}$ decreases from 5.05 nm at 1 mM to 4.64 nm at 50 mM. Fortunately, these slight spectral shifts seem to be the only effects of increasing the LR concentration up to 50 mM in PMMA. The overall spectral shape remains unchanged, as does the fluorescence lifetime, as shown in Figure 4b. In many other conjugated chromophores, aggregation at millimolar concentrations can lead to the formation of new electronic species (excimers or intermolecular exciton states) or a shortening of the fluorescence lifetime or both.[34] Previous work in our lab,[34] along with the data in Figure 4, shows that LR is relatively resistant to aggregation at concentrations up to 100 mM, allowing us to test a range of concentrations where intermolecular energy diffusion plays a significant role.

Time-Resolved Anisotropy in LR/PMMA Films. After a subset of the LR molecules in the PMMA host are excited by a linearly polarized laser pulse, they will undergo EET to neighboring LR sites. The loss of polarization memory in the sample due to this initial transfer step is reflected in the anisotropy decay.[38] The interchromophore transfer time can

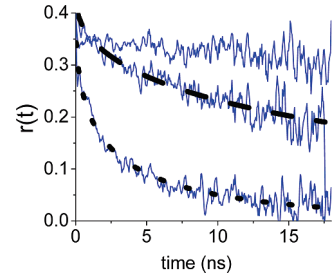

Figure 5. Time-resolved anisotropy decays for various LR concentrations in PMMA: 0.05 mM (control), 1.24 mM, $\tau_{pol} = 26.41$ ns (dashed line), and 4.45 mM, $\tau_{pol} = 2.38$ ns (dotted line). The τ_{pol} values are extracted by fitting the data with eq 5b, $r(t) = r_0 \exp[-(t/\tau_{pol})^{1/2}]$.

be estimated by measuring the fluorescence anisotropy decay $r(t)$, which takes the form of a stretched exponential due to the random distribution of acceptor LR molecules surrounding the initially excited LR molecule. We use two types of analytic functions to fit the experimental $r(t)$data

$$r(t) = 0.40 \exp\left[-\sqrt{\frac{t}{\tau_{pol}}}\right] + y_0 \tag{5a}$$

$$r(t) = r_0 \exp\left[-\sqrt{\frac{t}{\tau_{pol}}}\right] \tag{5b}$$

In eq 5a, we fix the initial amplitude of the decay to be the maximum theoretical value of 0.40 but allow the existence of a small residual offset y_0. This offset takes into account the fact that the long time $r(t)$ may not be exactly 0 due to slight variations in alignment or laser power. Equation 5b takes the opposite approach, assuming that $r(t)$ decay to 0 at long times but that the initial amplitude r_0 can vary. In practice, when fitting the data we find that the y_0 values range between 0.01 and 0.03 when using eq 5a, while the r_0 values range between 0.36 and 0.43 when using eq 5b. Note that $r_0 = 0.40$ is the expected value for a standard, single electronic state with a dipole-allowed transition. This value is commonly seen in perylene-based chromophores.[39] These different fitting strategies lead to slightly different τ_{pol} values, as discussed below. Experimental anisotropy decays for different LR concentrations are shown in Figure 5, along with fits obtained using eq 5b. As the chromophore concentration is increased, the decay becomes more rapid, and in all cases both eqs 5a and 5b do a reasonably good job of describing the dynamics. In order to connect the experimentally measured $r(t)$ to the parameters in eqs 2 and 3, we use a theoretical framework developed by Fayer and co-workers commonly referred to as GAF theory.[35,38] In this theoretical framework, $r(t)$ is directly proportional to $G_S(t)$, the survival probability of an excitation on a single site. $G_S(t)$ can be calculated using Greens functions and assuming that the EET rate is given by point-dipole Förster theory. $r(t)$ and the anisotropy decay time, τ_{pol}, can be found using the relations

$$G_s(t) = \frac{r(t)}{r_0} = \exp\left[\frac{-4}{3}\frac{\pi}{\sqrt{\lambda}}\Gamma\left(\frac{1}{2}\right)R_0^3 C_{LR}\sqrt{\frac{t}{\tau_{fl}}}\right] = \exp\left[-\sqrt{\frac{t}{\tau_{pol}}}\right] \tag{6}$$

$$\frac{1}{\tau_{pol}} = \left(\frac{4}{3}\frac{\pi}{\sqrt{\lambda}}\Gamma\left(\frac{1}{2}\right)R_0{}^3 C_{LR}\sqrt{\frac{1}{\tau_{fl}}}\right)^2 \quad (7)$$

where $\lambda = 2$ for donor-to-donor transport, $\gamma = 0.8452$, $\Gamma(x)$ is the gamma function with $\Gamma(1/2) = 1.7725 = \pi^{1/2}$, and $\tau_{fl} = 5.70$ ns. With all the constants in eq 7 evaluated, we find[40]

$$\tau_{pol} = 0.0508\frac{\tau_{fl}}{R_0{}^6 C_{LR}{}^2} \quad (8)$$

Equation 8 indicates that the anisotropy decay time τ_{pol} is proportional to $C_{LR}{}^{-2}$. Since $R_0{}^6$ also depends on C_{LR} as indicated in Figure 4, it is necessary to plot the product $\tau_{pol}R_0{}^6$ versus C_{LR} in order to see its true concentration dependence. A log−log plot of these two quantities should result in a slope of −2 according to eq 8. The log−log plots of the experimental data points are shown in Figure 6. When eq 5a is used and r_0 is fixed at 0.40 during the fittings, the data in Figure 6a yield a slope of -1.90 ± 0.11. When eq 5b is used to fit the anisotropy decays, the data in Figure 6b yield a slope of -1.54 ± 0.13. It turns out that this discrepancy in the slope is an artifact arising from the fact that eq 5b does not do a good job of fitting the 50 mM anisotropy decay. When the 50 mM point is excluded from the linear fits, the data in Figure 6a yield a slope of -2.11 ± 0.16 while the data in Figure 6b give a slope of -1.91 ± 0.17. The point of this discussion is to emphasize that the slope of −2 is robust with respect to the data fitting methodology. We can say with confidence that once the concentration dependence of $R_0{}^6$ is properly taken into account, the $C_{LR}{}^{-2}$ dependence of τ_{pol} predicted by eq 8 is confirmed to within the experimental error of ±10%. This dependence of τ_{pol} on chromophore concentration has been observed previously in polymer and glass systems.[41,42]

The next question is whether eq 8 correctly predicts the magnitude of τ_{pol}, in addition to its concentration dependence. If we assume the concentration dependence to be strictly $C_{LR}{}^{-2}$, we can plot the quantity $\tau_{pol}R_0{}^6$ versus $C_{LR}{}^{-2}$. When τ_{pol} values obtained from eq 5a fits are used, the plot shown in Figure 7a with a slope of 0.18 ± 0.01 is obtained when the y-intercept is fixed at 0. With the τ_{pol} values obtained from eq 5b fits to the anisotropy decays, the plot shown in Figure 7b yields a straight line whose slope is found to be 0.26 ± 0.02 when the y-intercept is fixed at 0. For both plots, we also show the theoretically predicted line based on eq 8. Exclusion of the 50 mM point from either eq 5a or 5b fit data had no effect on these slopes to within the error. The experimental values derived from both fitting options are in decent agreement with the theoretical slope of 0.29 obtained from eq 8 with $\tau_{fl} = 5.7$ ns. This agreement is not too surprising in light of the fact that a large difference between the experimental and theoretical values would have resulted in a visible offset between the experimental and theoretical lines in Figure 6. If anything, it appears that theory slightly underestimates the decrease in τ_{pol} values as C_{LR} is increased. To summarize, the LR anisotropy data show that not only does the simple GAF theory provide a good qualitative description of the initial EET dynamics, it is nearly quantitative as well, with the theoretically predicted τ_{pol} values differing from the experimental values by only about 10−30%.

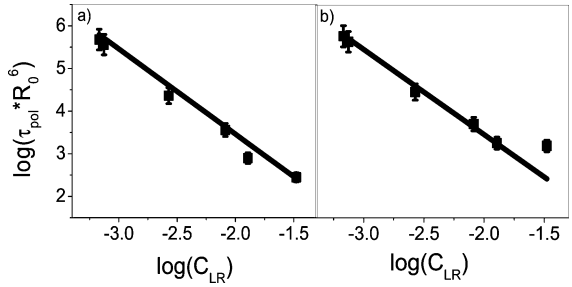

Figure 6. (a) log−log plots of anisotropy decay time τ_{pol}, as extracted using eq 5a, scaled by the concentration-dependent Förster radius. (b) Same as (a), but using eq 5b to extract τ_{pol}. Also shown on both plots is the predicted dependence according to eq 8 where $y = -2.00x - 0.54$ (solid line).

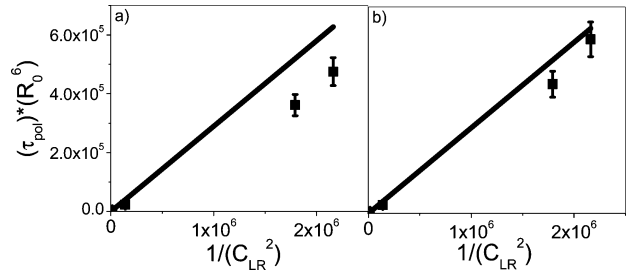

Figure 7. (a) Linear plot of anisotropy decay time τ_{pol}, as extracted using eq 5a, scaled by the concentration-dependent Förster radius. (b) Same as (a), but using eq 5b to extract τ_{pol}. Also shown on both plots is the predicted dependence according to eq 8 $y = -0.29x$ (black line).

Time-Resolved Fluorescence Quenching in LR Mixed with R700 and MG. It should be emphasized that the anisotropy decay only measures the initial hopping event in EET.[38] For concentrated systems, many subsequent hops may occur during the molecule's excited-state lifetime. To measure the dynamics of this longer time energy migration, we turn to fluorescence quenching. We use the organic dyes R700 and MG as acceptors, since both have strong absorptions that overlap well with LR's fluorescence as shown in Figure 2. Experimentally, both molecules quench the LR fluorescence, and this quenching is accompanied by a rapid growing in of the acceptor fluorescence, consistent with what is expected for EET-mediated quenching. Also consistent with expectations, as C_{LR} is increased, the LR fluorescence decay becomes more rapid due to quenching facilitated by exciton diffusion.

In order to simplify our data analysis, we chose a relatively simple analytical expression that divides the quenching into two different terms and minimizes the number of free parameters. Both experimental and theoretical considerations suggest that the donor decay in the presence of an acceptor should have the general form[43]

$$I_D(t) = I_D(0)\exp\left[-\frac{t}{\tau_{fl}} - At - B\sqrt{t}\right] \quad (9)$$

The A term represents the contribution due to hopping of the excitation from donor to donor, while the B term represents a single step transfer of energy directly from an excited donor to a nearby acceptor without intervening hops. To connect A and B to the parameters of Förster theory, we follow the formulation of Jang et al.[16] where an approximate expression for the donor fluorescence lifetime is derived, similar to the approach of Gösele et al.[44]

$$A = 4\pi D\sigma_F C_A \quad (10)$$

$$B = \frac{4}{3}\pi {R_{DA}}^3 C_A \sqrt{\pi k_{fl}} \tag{11}$$

In eqs 10 and 11, D is the exciton diffusion constant through the material, σ_F is the quenching radius of the acceptor, C_A is the acceptor concentration in molecules/volume, R_{DA} is the donor → acceptor Förster radius, and $k_{fl} = 1/\tau_{fl}$ is the excited-state decay rate. For our experiments, the donor is LR, while the acceptor is either R700 or MG. We note that only the A term depends on D, which in turn depends on the donor concentration C_D. The B term is independent of donor concentration and for low values of C_D, it should dominate the behavior of $I_D(t)$. If we fix C_A and then divide the variable C_D decays by the low C_D decay, we find

$$\frac{I(t)[\text{high } C_{LR}]}{I(t)[\text{low } C_{LR}]} = \frac{\exp[-k_{fl}t - At - B\sqrt{t}]}{\exp[-k_{fl}t - B\sqrt{t}]} = \exp[-At] \tag{12}$$

In other words, by ratioing the variable C_D decays to the intrinsic decay at negligible C_D, we can isolate the A term that reflects exciton diffusion.[45] We find experimentally that $C_{LR} = C_D = 10^{-4}$ M is low enough that donor-to-donor hopping can be neglected. This can be seen from Figure 5, where the 0.05 mM LR anisotropy decay is flat to within the experimental error and also by the fact that using 1×10^{-4} and 1×10^{-5} M concentrations as the "low C_{LR}" decay in eq 12 yielded the same results for the A term to within the experimental error. In practice, we used the 1×10^{-4} M decay curve when analyzing the data since it had the best signal-to-noise and thus yielded the cleanest ratio decay for the extraction of A. Figure 8 shows the ratio decays for different LR concentrations while the acceptor concentration is held fixed at 2 and 4 mM for the cases of R700 and MG, respectively. Also shown are the exponential fits for the ratioed decays in accordance with eq 12. For both MG and R700, the quenching rate increases as C_{LR} is increased, and all the decays can be fit reasonably well using a single exponential. In this way, we can obtain A as a function of C_{LR}.

Dependence of *A* Term on LR Concentration. In order to compare the experimental dependence of A on C_{LR} to theoretical predictions, we need to consider how the parameters D and σ_F depend on concentration. If we assume σ_F is constant, then only D depends on C_{LR}, with a 4/3 power law as given in eq 2. More sophisticated theories take into account

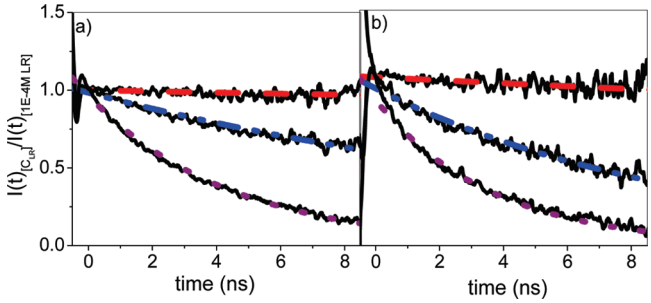

Figure 8. (a) Experimental quenching decays as obtained using eq 12 for the acceptor R700 concentration of 2 mM with (red dashed line) 1 mM LR ($A^{-1} = 262.23$ ns), (blue dash dotted line) 5 mM LR ($A^{-1} = 18.18$ ns), and (purple dotted line) 20 mM LR ($A^{-1} = 4.45$ ns). (b) Same as in (a) but with the acceptor MG concentration of 4 mM, with (red dashed line) 1 mM LR ($A^{-1} = 109.73$ ns), (blue dash dotted line) 5 mM LR ($A^{-1} = 9.69$ ns), (purple dotted line) 20 mM LR ($A^{-1} = 3.62$ ns).

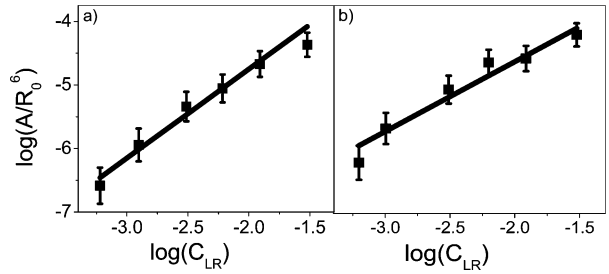

Figure 9. (a) log−log plot of the decay constant A, scaled by the concentration-dependent Forster radius, versus C_{LR} with the acceptor R700 concentration set to 2 mM. The line represents the linear least-squares fit with slope = 1.2 ± 0.2. (b) log−log plot of the decay constant A, scaled by the concentration-dependent Forster radius, versus C_{LR} with the acceptor MG concentration set to 4 mM. The line represents the linear least-squares fit with slope = 1.1 ± 0.2.

the fact that σ_F can also depend on D. Again, following the treatment of Jang et al.[16,46]

$$\sigma_F \cong R_{DA}\frac{\Gamma(0.75)}{2\Gamma(1.75)}\left(\frac{k_S {R_{DA}}^2}{D}\right)^{1/4} = 0.676\left(\frac{k_S {R_{DA}}^6}{D}\right)^{1/4} \tag{13}$$

If we now take D to be given by eq 2, we find that $A \propto {C_D}^{1.00}$ rather than $A \propto {C_D}^{1.33}$. Figure 9 is a log−log plot of the A term, scaled by the changing ${R_0}^6$ values, versus C_{LR}. The plot yields a power law dependence of 1.2 ±0.2 for R700 and 1.1 ±0.2 for MG. It is reassuring that the values for both acceptors are similar, despite the fact that these molecules have very different chemical structures. Our data are closer to the $A \propto {C_D}^{1.33}$ dependence, although the error in the slope is sufficiently large that it is difficult to definitely conclude which dependence is correct. Nevertheless, we can say that the simple theory in eqs 2 and 9 predicts the qualitative behavior of the fluorescence quenching as a function of C_{LR}, similar to the case for the anisotropy decay. The ${C_D}^{1.33}$ dependence of the excitation diffusion constant has been previously observed over a limited concentration range in both liquid solutions[47] and doped polymers.[48]

Values for *D* Calculated Using Various Theories. Equations 6−8 do a good job describing not only the trend of the anisotropy decay time τ_{pol} with C_{LR} but also its absolute magnitude. In a similar vein, we can ask whether the theoretical approach embodied in eqs 9−11 can quantitatively predict the decay rate of $I_D(t)$. In particular, we are interested in whether the value of D obtained from analysis of the quenching decays agrees with that calculated from eq 2. In the following discussion, we will concentrate on the $C_{LR} = 10$ mM case, where D is relatively large, and consider only the data where R700 was used as an acceptor. We first consider two theoretical estimates for D. The first is to use eq 2 where $\eta = 0.56$ (Jang's theory) or $\eta = 0.43$ (GAF theory). This results in a predicted $D = 8.56$ nm^2/ns or 6.57 nm^2/ns when ${R_0}^{LR\rightarrow LR} = 4.77$ nm and $C_{LR} = 10$ mM.

An alternate method is to assume that there exists an average hopping time for the excitation, τ_{hop}, and that the average distance between LR sites is l_{hop}. In this case, the diffusion constant can be estimated using the well-known equation

$$D = \frac{1}{6}\frac{{l_{hop}}^2}{\tau_{hop}} \tag{14}$$

The problem is then estimating the quantities l_{hop} and τ_{hop}. For a cubic lattice, the average distance between chromophores is just the cube root of the density.[43]

$$l_{hop} = \frac{1}{\sqrt[3]{C_{LR}}} \tag{15a}$$

while for an isotropically disordered system, it can be shown that the average distance between chromophores leads to[49]

$$l_{hop} = \Gamma(4/3)\sqrt[3]{\frac{3}{4\pi C_{LR}}} = \frac{0.554}{\sqrt[3]{C_{LR}}} \tag{15b}$$

For τ_{hop}, we have two choices. The first is to take $\tau_{hop} = \tau_{pol}$. For $C_{LR} = 10$ mM, the average anisotropy decay time at this concentration $\tau_{pol} = \tau_{hop} = 0.4$ ns. The second choice is to take $\tau_{hop} = \tau_{FRET}$, which is calculated using eq 1a with $R = l_{hop}$. Clearly eq 15b is the more appropriate way to estimate l_{hop}, although eq 15a has also previously been applied to amorphous solids.[50] For $C_{LR} = 1 \times 10^{-2}$ M, we find $l_{hop} = 3.1$ nm, and thus $D = 4.0$ nm^2/ns ($\tau_{hop} = \tau_{pol} = 0.4$ ns) or 3.7 nm^2/ns ($\tau_{hop} = \tau_{FRET} = 0.43$ ns). It should be noted that if we naively used Equation 15a to calculate $l_{hop} = 5.5$ nm, the results would be very different: $D = 12.6$ nm^2/ns ($\tau_{hop} = \tau_{pol} = 0.4$ ns) or 0.4 nm^2/ns ($\tau_{hop} = \tau_{FRET} = 13.4$ ns). The nonlinear dependence of eqs 1a and 14 on l_{hop} means that small changes in assumptions about intermolecular spacing can have large effects on the estimated diffusion constant and length.

Estimating *D* from Experimental Data. The next question is whether the values of D predicted theoretically in the preceding section are consistent with values obtained from analysis of the experimental quenching data. Extracting quantitative values for D from the fluorescence quenching experiments is problematic due to the presence of two unknowns in the A term: D and σ_F. The most straightforward approach is to naively assume that the quenching radius $\sigma_F = R_{DA}$. In this case, since we know all the other parameters in A, it is straightforward to extract the diffusion constant as a function of C_{LR}. Using the data in Figure (9), we find that $A = 44.6{C_{LR}}^{1.2}$ ns^{-1} when $C_A = C_{R700} = 2$ mM and where C_{LR} is in units of molecules/nm.[3] Using this relation, we can calculate that $A = 0.079$ ns^{-1} when $C_{LR} = 10$ mM. Given $\sigma_F = {R_0}^{LR\rightarrow R700} = 5.85$ nm, we can use eq 10 to solve for $D = 0.89$ nm^2/ns. This value of D results in $L_D = 5.52$ nm.

A more sophisticated approach is to use Jang's estimate of σ_F in eq 13 and assume a linear dependence of A on C_{LR}. Even though this contradicts the power law dependence seen in the data in Figure 9, we can assume that uncertainties in the power law are large enough that the $A \propto {C_D}^{1.00}$ case is worth examining. Using eq 13 and Jang's expression for D in a solid system, we add a scaling factor β to take into account the possibility that the actual value of D is different from that predicted by eq 2.

$$D = 0.56\left(\frac{4\pi}{3}C_D\right)^{4/3}\frac{\beta {R_{DD}}^6}{\tau_{fl}} \tag{16}$$

Using eqs 11, 13, and 14, we can then find an analytical expression for A scaled by R_{DD}

$$\frac{A}{{R_{DD}}^{9/2}} = \frac{23.04{R_{DA}}^{3/2}\beta^{3/4}C_A}{\tau_{fl}}C_D \tag{17}$$

A plot of $A/{R_{DD}}^{9/2}$) versus C_{LR} is shown in Figure 10 and results in a slope of 0.016. In order to obtain this experimental slope given all the other constants in eq 17, we find that $\beta = 0.14$ is required. When this value for β is plugged back into eq 16, we obtain a value for $D = 1.23$ nm^2/ns and $L_D = 6.5$ nm when $C_{LR} = 10$ mM. The physical reason why this value of D is larger is that eq 13 assumes that σ_F decreases as D increases. Thus to obtain the same amount of quenching, a larger value for D is required.

The two approaches outlined above rely on assumptions about molecular parameters like σ_F. A different approach, based only on experimentally derived quantities that avoids the problem of estimating σ_F, has been suggested by Powell and Soos.[43] If we examine eqs 10 and 11, we can see that if both A and B terms are known, it is possible to derive an expression for D purely in terms of these two decay rates

$$D = 0.2196\left(\frac{a^2}{b}\right)^{2/3} \tag{18}$$

where $A = aC_A$ and $B = bC_A$. In fact, this type of relation can be derived from many different theories of fluorescence quenching, including the simple Chandreshankar diffusion model[51,52]

$$D = 0.1263\left(\frac{a^2}{b}\right)^{2/3} \tag{19}$$

and the related model of Ali et al.[53]

$$D = 0.2005\left(\frac{a^2}{b}\right)^{2/3} \tag{20}$$

A similar relation can also be derived from a lattice hopping model developed to describe EET in molecular crystals.[51] Rather than relying on knowledge of quantities like R_{DD}, R_{DA}, and σ_F, we now only have to assume one of the proportionality constants in eqs 18−20. As stated above, we found $A = 44.6{C_{LR}}^{1.2}$ when $C_{R700} = 2$ mM, from which we can obtain a value for a for any value of C_{LR}, and in particular find $a = 66$ ns^{-1} nm^3 for $C_{LR} = 10$ mM. To find b, we must do the complementary experiment where the donor concentration is held constant and the acceptor concentration is varied. Since we know A and τ_{fl}, we can use eq 9 to fit the decays, with B as the only adjustable parameter. Figure 11 shows the $I_D(t)$ decays for fixed $C_{LR} = 10$ mM and variable C_{R700}, along with fits using eq 9 with $A = aC_{R700}$, and $\tau_{fl} = 5.7$ ns. The only remaining adjustable parameter is B, which is extracted using least-squares fitting of the decays at various values of C_{R700}. The extracted B values can then be plotted versus C_{R700} as shown in Figure 12. The slope of a linear fit to this data yields $b = 1060 \pm 50$ ns$^{-0.5}$ nm^3. We can now evaluate both a and b parameters for any values of C_{LR} and C_{R700}. Using values for a and b when $C_{LR} = 10$ mM, along with eqs 18−20, we find that $D = 0.32-0.56$ nm^2/ns. These values are lower than the estimates derived from eq 2, and also lower than the values derived in the preceding paragraph where different values for σ_F were assumed. The tendency of this approach to predict lower D values has been noted previously.[43] Unfortunately, this approach is still model-dependent and only provides a range of

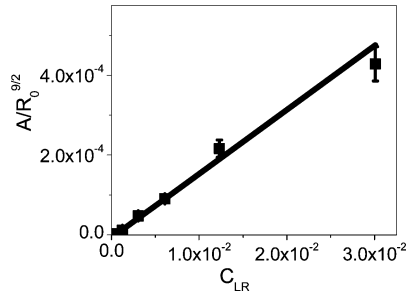

Figure 10. Plot of the diffusional quenching constant A term, scaled by the concentration-dependent Förster radius, versus C_{LR}. The line represents the linear least-squares fit with slope = 0.016.

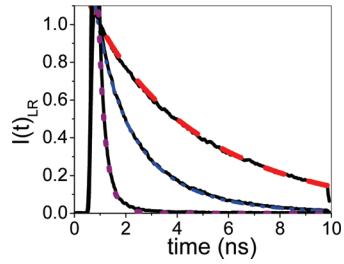

Figure 11. Fluorescence decays of LR with $C_{LR} = 10$ mM and variable C_{R700} acceptor concentrations. The data are fit using eq 9 with $\tau_{fl} = 5.70$ ns, $A = a\,C_{R700}$ (where $a = 66$ ns^{-1}), and by varying B. The data and fits are as follows: (red dash lines) 10^{-4}M R700 with 10 mM LR ($B = 0.156$ ns$^{M-0.5}$), (blue line) 2 mM R700 with 10 mM LR ($B = 0.972$ ns$^{-0.5}$), and (red dotted line) 10 mM R700 with 10 mM LR ($B = 6.625$ ns$^{-0.5}$).

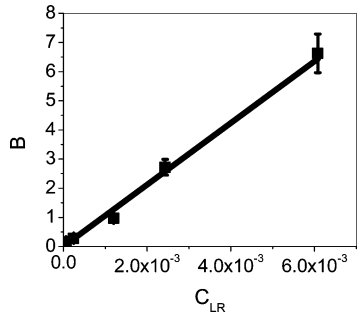

Figure 12. Plot of B term from eq 9 versus C_{R700}, the concentration of the quencher Rhodamine 700. The line represents the linear least-squares fit with slope = 1060 ns$^{-0.5}$ nm^3.

TABLE 1: D and L_D for 10 mM Lumogen Red in PMMA Based on Various Theories and Experimental Analysis of Fluorescence Quenching Data[a]

method for estimating D	D (nm^2/ns)	L_D (nm)
theory, eq 2, $\eta = 0.56$	8.56	17.1
theory, eq 2, $\eta = 0.43$	6.57	15.0
theory, eqs *14* and *15b*, $\tau_{hop} = \tau_{pol}$	4.0	11.7
theory, eqs *14*, *15b*, $\tau_{hop} = \tau_{FRET}$	3.7	11.2
experimental, $\sigma_F = R_{DA}$	0.89	5.5
experimental, eqs *16* and *17*	1.20	6.4
experimental, eq *18*	0.56	4.4
experimental, eq *19*	0.32	3.3
experimental, eq *20*	0.51	4.2

[a] L_D is calculated using eq 3 and assuming a fluorescence lifetime of 5.70 ns in the absence of any acceptors.

values for D. Nevertheless, it confirms that the experimental values for D are significantly less than those predicted by analytical theories based on eq 2. Table 1 summarizes the theoretical and experimental values for D, along with L_D values calculated using eq 3 for the case of a 10 mM LR film without quenchers at $\tau_{fl} = 5.70$ ns. In the presence of quenchers, τ_{fl} would decrease and thus L_D would be smaller.

Discussion

The results in Table 1 show that three different approaches to recover D from the experimental fluorescence quenching data all lead to similar results. This indicates the robustness of the overall approach. The experimentally derived D values range from 0.32 to 1.20 nm^2/ns, but all are substantially less than the values of $D \sim 3.7-8.6$ nm^2/ns estimated from either the analytic expression in eq 2 or the anisotropy analysis in conjunction with eqs 14. We now consider four possible origins of this discrepancy.

1. Nonrandom Distributions of Donor and/or Acceptor Molecules. One possible explanation is that the donor and acceptor molecules are not uniformly distributed within the PMMA host. Previously, deviations from Förster theory at low concentrations have been observed and ascribed to clustering of ionic donor and acceptor dyes in a polymer matrix.[54] Using Monte Carlo simulations, it has been shown that nonrandom chromophore distributions can both accelerate and retard energy migration, depending on the type of clustering.[55,56] If donors and acceptors cluster together, this would result in enhanced EET between donors and acceptors, the opposite of what is observed here. To explain our results, the clustering would have to be between dyes of the same molecular structure. For example, if the R700 molecules cluster together, their effective concentration around individual LR donors will decrease and the average distance that an excitation has to travel will increase. A similar problem would occur if the LR donors were clustered together. Such LR clustering might also help to explain the solvatochromic shifts seen in the LR/PMMA spectra, as well as the fact that the τ_{pol} values are actually slightly shorter than those predicted by the point-dipole Förster theory. On the other hand, if any clustering were present, it must be fairly weak, since the molecules are not close enough for either their spectral shape or fluorescence lifetime to be affected. No evidence of phase separation or inhomogeneous distribution could be seen when the films were examined under a microscope, although such clustering would probably occur on much smaller length scales than those accessible by optical microscopy. Dielectric and thermal measurements on LR in PMMA indicate that strong guest−host interactions exist, which would be expected to work against clustering.[57,58] Additional evidence against the role of LR clustering is the fact that the dependences of both the anisotropy decay and fluorescence quenching on C_{LR} do not exhibit anomalous behavior, except perhaps at the highest concentrations (e.g., the 50 mM point in Figure 10). At higher values of C_{LR}, where the average intermolecular distance approaches 2 nm, one might expect that clustering would lead to deviations from the expected $\tau_{pol} \propto C_{LR}^{-2}$ and $A \propto C_{LR}^{-4/3}$ dependences. Although the data in Figures 6 and 9 are too noisy to conclusively rule out small deviations, such deviations are certainly not a dominant effect. A final piece of evidence against the formation of quasi-ordered clusters of LR is the rapid anisotropy decay observed at all values of C_{LR} that agrees well with that predicted theoretically. A cluster with locally ordered LR molecules would likely exhibit a slower anisotropy decay than expected, since EET to a neighboring molecule with similar orientation would not depolarize the fluorescence. Finally, we are unaware of any previous observations of such loose clusters of weakly interacting molecules in polymer hosts. Certainly entropic considerations would make such clustering unlikely from a free energy standpoint.

2. Breakdown of the Point-Dipole Approximation. A second concern is whether FRET theory is sufficient to predict the EET rates. All our estimates rely on the point dipole−dipole expressions for describing the EET process. This approximation is known to break down for small chromophore separations, and improved expressions have been derived by a variety of workers.[59−65] At this point, however, there is no sign that this is occurring in our data. The average separation between molecules is much greater than a molecular diameter even at the highest concentrations. Furthermore, the good agreement between the GAF theory, which assumes point-dipole interactions, and the anisotropy data suggests that any nonidealities in the intermolecular interaction term should be relatively small. If simple FRET theory describes the early time dynamics correctly, there is no reason to suspect that more complicated expressions would be required for energy transfer at later points in the exciton's lifetime.

3. Acceptor Perturbation of Exciton Diffusion. One assumption inherent in our analysis is that the diffusion constant estimated from experiments on LR-only films can be applied to mixed films containing both LR and an energy acceptor. Put another way, we assume that the presence of the acceptor does not perturb energy migration through the LR molecules. As discussed earlier in the context of eqs 10 and 13, there is always some uncertainty in σ_F, the donor−acceptor quenching radius. But it is also possible that the presence of the acceptor molecules changes the EET rate between the LR molecules themselves (D in eq 10), for example by changing the local refractive index or excluded volume effects. This latter effect has recently been explored using Monte Carlo simulations.[66] It was found that nonzero excluded volumes of donor and acceptor molecules could lead to a small but noticeable slowdown in the $G_S(t)$ decay of the donors. Such excluded volume effects can also be taken into account in analytical theories, but at the cost of introducing additional parameters.[16] The effect of a nonspherical molecular shape would introduce even more complexity. A detailed attempt to treat this possible effect is beyond the scope of this paper. For now, we can only say that such an effect would go in the right direction, reducing the apparent exciton diffusion derived from the quenching experiments in mixed films. We have tried to address this concern through the use of both R700 and MG as chemically distinct acceptors that yield very similar behaviors. But since both are salts with roughly similar size and dimensions, it is possible that their perturbative effects on the exciton diffusion would also be similar. One way to determine the importance of acceptor-perturbed exciton diffusion would be to compare the experimental data to high-level simulations of the EET that take the molecular-level structure into account.[67−71] If this type of effect is found to be important, then eq 2 is not valid when energy migration occurs in the presence of acceptors, since D would depend on the molecular structure and concentration of the acceptor.

4. Disorder-Induced Anomalous Diffusion. The GAF theory correctly predicts τ_{pol} but overestimates the D obtained from the fluorescence quenching experiments, as do the other theoretical models described in the previous section. Many experimental studies on fluorescence quenching[43,46,48,72] rely on analytical expressions[18,43,44,53,73−76] that assume that the diffusion constant D is truly constant—it does not change over the course of the exciton lifetime. A fundamental question is whether any theoretical approach that relies on a single diffusion constant D can adequately describe the energy migration at all times. In fact, it has long been recognized that approximate analytical expressions like those in eqs 9−11 or eqs 14 fail to capture the complexity of energy transfer in the presence of diffusion through a random environment. There are many experimental studies that indicate that dispersive transport, which leads to anomalous diffusion, plays an important role in organic solids.[77−83] Numerical simulations have shown that the excitation hopping rate may not be constant in systems with orientational and energetic disorder, leading to anomalous (time-dependent) exciton diffusion dynamics.[84−89]

Several different types of sophisticated analytical theories have been developed to take this nonideal situation into account.[12−14,16,90−99] These approaches have had some success in describing experimental results in both liquid solutions[46,100,101] and disordered solids.[102−106] The discrepancy between the exciton diffusion rate surmised from experiments sensitive to early time dynamics (anisotropy) as opposed to those that reflect motion over the exciton's entire lifetime (quenching) in disordered systems may be ascribed to the breakdown of the constant diffusion model. After the initial hop, which determines the anisotropy decay rate, there may be a slowdown of the EET over subsequent transfer events due to factors like a nonrandom distribution of chromophores within the host material or energetic and orientational disorder or some combination of these factors. The relative importance of different types of disorder, for example, orientational versus energetic, remains to be determined. Photon echo measurements on dyes dissolved in PMMA have indicated values up to several hundred wavenumbers for the width of the static energy distribution.[107−112] Such values are within the range expected to significantly affect exciton motion.[86] The development of new models to reproduce our experimental results is beyond the scope of this paper. Recently a relatively simple model for exciton diffusion in energetically disordered materials has been developed,[113] and it may be applicable to the current system. For now, we simply state the empirical fact that our data are consistent with the idea that static disorder in an amorphous polymer can lead to a significant slowing down of the exciton motion over the course of its excited-state lifetime.

Conclusion

The work in this paper shows that the sterically congested perylenediimide dye LR is a suitable chromophore for testing the dynamical predictions of simple Förster-type exciton diffusion theory. Many earlier experiments were performed on neat solids where there was no way to vary the donor concentration and confirm true Förster type behavior, without complications from trapping species, etc. The LR/PMMA system provides a very clean model with which to test the limitations of simple diffusion theory as applied to exciton motion. Our results indicate that it may break down in this system. We find that this theory does a good job of describing the concentration dependence of both the anisotropy decays and the fluorescence quenching at chromophore densities of up to 50 mM in a PMMA polymer host. Standard GAF theory leads to estimates of the anisotropy decay time τ_{pol} that are in almost quantitative agreement with experiment. In contrast, the extension of this theory to predict values of D results in an overestimation of the experimentally derived value by almost an order of magnitude, although the expected behavior with chromophore concentrations is reproduced. We have discussed several possible reasons for this discrepancy. Most analytical theories considered in this paper have a high sensitivity to input parameters, like the average chromophore spacing, that makes a quantitative comparison to experiment difficult. It seems likely that this problem can be resolved through the use of high-level Monte Carlo simulations of energy migration through a realistic molecular environment, a challenging task. But the LR/PMMA system is a good candidate for studying this phenomenon in

conjunction with such simulations due to the lack of aggregation at high concentrations. This system may also be of interest from a practical standpoint. While the values of $L_D = 3.3-6.4$ nm extrapolated from experiment are smaller than theoretically predicted, it is encouraging that they are relatively large even at $C_{LR} = 10$ mM. In principle, if the quasi-linear scaling observed in Figure 9 holds at higher concentrations, and if concentration quenching of LR's excited state lifetime can somehow be circumvented, then increasing C_{LR} by a factor of 100 to 1 M should result in L_D values of up to 50 nm, on the order of what is attainable using incoherent hopping transport in highly ordered systems.[114] Experiments on higher concentration samples are currently underway.

Acknowledgment. We acknowledge support by the National Science Foundation, Grant Number CHE-0719039.

References and Notes

(1) Friend, R. H.; Gymer, R. W.; Holmes, A. B.; Burroughes, J. H.; Marks, R. N.; Taliani, C.; Bradley, D. D. C.; Santos, D. A. D.; Bredas, J. L.; Logdlund, M.; Salaneck, W. R. Electroluminescence in conjugated polymers. *Nature* **1999**, *397*, 121–128.

(2) Brabec, C. J.; Sariciftci, N. S.; Hummelen, J. C. Plastic solar cells. *Adv. Funct. Mater.* **2001**, *11*, 15–26.

(3) Gregg, B. A. Excitonic solar cells. *J. Phys. Chem. B* **2003**, *107*, 4688–4698.

(4) McQuade, D. T.; Pullen, A. E.; Swager, T. M. Conjugated polymer-based chemical sensors. *Chem. Rev.* **2000**, *100*, 2537–2574.

(5) Möbius, D.; Kuhn, H. Energy transfer in monolayers with cyanine dye Sheibe aggregates. *J. Appl. Phys.* **1988**, *64*, 5138–5141.

(6) Jang, S.; Newton, M. D.; Silbey, R. J. Multichromophoric Förster resonance energy transfer. *Phys. Rev. Lett.* **2004**, *92*, 218301/1−218301/4.

(7) Beljonne, D.; Hennebicq, E.; Daniel, C.; Herz, L. M.; Silva, C.; Scholes, G. D.; Hoeben, F. J. M.; Jonkheijm, P.; Schenning, A. P. H. J.; Meskers, S. C. J.; Phillips, R. T.; Friend, R. H.; Meijer, E. W. Excitation migration along oligophenylenevinylene-based chiral stacks: delocalization effects on transport dynamics. *J. Phys. Chem. B* **2005**, *109*, 10594–10604.

(8) Didraga, C.; Malyshev, V. A.; Knoester, J. Excitation energy transfer between closely spaced multichromophoric systsm: effects of band mixing and intraband relaxation. *J. Phys. Chem. B* **2006**, *110*, 18818–18827.

(9) Ahn, T. S.; Thompson, A. L.; Bharathi, P.; Muller, A. M.; Bardeen, C. J. Light-harvesting in carbonyl-terminated phenylacetylene dendrimers: the role of delocalized excited states and the scaling of light-harvesting efficiency with dendrimer size. *J. Phys. Chem. B* **2006**, *110*, 19810–19819.

(10) Beljonne, D.; Curuchet, C.; Scholes, G. D.; Silbey, R. J. Beyond Förster resonance energy transfer in biological and nanoscale systems. *J. Phys. Chem. B* **2009**, *113*, 6583–6599.

(11) Förster, T. *Ann. Phys.* **1948**, *2*, 55.

(12) Haan, S. W.; Zwanzig, R. Förster migration of electronic excitation between randomly distributed molecules. *J. Chem. Phys.* **1978**, *68*, 1879–1883.

(13) Gochanour, C. R.; Andersen, H. C.; Fayer, M. D. Electronic excited state transport in solution. *J. Chem. Phys.* **1979**, *70*, 4254–4271.

(14) Loring, R. F.; Andersen, H. C.; Fayer, M. D. Electronic excited state transport and trapping in solution. *J. Chem. Phys.* **1982**, *76*, 2015–2027.

(15) Rieger, P. T.; Palese, S. P.; Miller, R. J. D. On the Förster model: computational and ultrafast studies of electronic energy transport. *Chem. Phys.* **1997**, *221*, 85–102.

(16) Jang, S.; Shin, K. J.; Lee, S. Effects of excitation migration and translational diffusion in the luminescence quenching dynamics. *J. Chem. Phys.* **1995**, *102*, 815–827.

(17) Cross, A. J.; Fleming, G. R. Analysis of time-resolved fluorescence anisotropy decays. *Biophys. J.* **1984**, *46*, 45–56.

(18) Lakowicz, J. R. *Principles of Fluorescence Spectroscopy*, 2nd ed.; Kluwer Academic: New York, 1999.

(19) Würthner, F. Perylene bisimide dyes as versatile building blocks for functional supramolecular architectures. *Chem. Commun.* **2004**, 1564–1579.

(20) Langhals, H. Control of the interactions in multichromophores: Novel concepts. Perylene bis-imides as components for larger functional units. *Helv. Chim. Acta* **2005**, *88*, 1309–1341.

(21) Horowitz, G.; Kouki, F.; Spearman, P.; Fichou, D.; Nogues, C.; Pan, X.; Garnier, F. Evidence for n-type conduction in a perylene tetracarboxylic diimide derivative. *Adv. Mater.* **1996**, *8*, 242–245.

(22) Ferrere, S.; Zaban, A.; Gregg, B. A. Dye sensitization of nanocrystalline tin oxide by perylene derivatives. *J. Phys. Chem. B* **1997**, *101*, 4490–4493.

(23) Kim, J. Y.; Bard, A. J. Organic donor/acceptor heterojunction photovoltaic devices based on zinc phthalocyanine and a liquid crystalline perylene diimide. *Chem. Phys. Lett.* **2004**, *383*, 11–15.

(24) Keivanidis, P. E.; Howard, I. A.; Friend, R. H. Intermolecular interactions of perylene diimides in photovoltaic blends of fluorene copolymers: disorder effects on photophysical properties, film morphology and device efficiency. *Adv. Funct. Mater.* **2008**, *18*, 3189–3202.

(25) Seybold, G.; Wagenblast, G. New perylene and violanthrone dyestuffs for fluorescent collectors. *Dyes Pigm.* **1989**, *11*, 303–317.

(26) Swift, P. D.; Smith, G. B. Color considerations in fluorescent solar concentrator stacks. *Appl. Opt.* **2003**, *42*, 5112–5117.

(27) Sark, W. G. J. H. M. v.; Barnham, K. W. J.; Sloof, L. H.; Chatten, A. J.; Buchtemann, A.; Meyer, A.; McCormack, S. J.; Koole, R.; Farrell, D. J.; Bose, R.; Bende, E. E.; Burgers, A. R.; Budel, T.; Quilitz, J.; Kennedy, M.; Meyer, T.; Donega, C. D. M.; Meijeriink, A.; Vanmaekelbergh, D. Luminescent solar concentrators—a review of recent results. *Opt. Express* **2008**, *16*, 21773–21792.

(28) Rowan, B. C.; Wilson, L. R.; Richards, B. S. Advanced material concepts for luminescent solar concentrators. *IEEE Sel. Top. Quantum Electron.* **2008**, *14*, 1312–1322.

(29) Reisfeld, R.; Gvishi, R.; Burshtein, Z. Photostability and loss mechanism of solid state red perylimide dye lasers. *J. Sol-Gel Sci. Technol.* **1995**, *4*, 49–55.

(30) Sheridan, A. K.; Buckler, A. R.; Fox, A. M.; Bacher, A.; Bradley, D. D. C.; Samuel, I. D. W. Efficient energy transfer in organic thin films—implications for organic lasers. *J. Appl. Phys.* **2002**, *92*, 6367–6371.

(31) García-Moreno, I.; Costela, A.; Martin, V.; Pintado-Sierra, M.; Sastre, R. Materials for reliable solid-state dye laser at the red spectral edge. *Adv. Funct. Mater.* **2009**, *19*, 1–6.

(32) Ranke, P.; Bleyl, I.; Simmerer, J.; Haarer, D.; Bacher, A.; Schmidt, H. W. Electroluminescence and electron transport in a perylene dye. *Appl. Phys. Lett.* **1997**, *71*, 1332–1334.

(33) Sliwa, M.; Flors, C.; Oesterling, I.; Hotta, J.; Müllen, K.; Schryver, F. C. D.; Hofkens, J. Single perylene diimide dendrimers as single-photon sources. *J. Phys.: Condens. Matter* **2007**, *19*, 445004/1–445005/14.

(34) Al-Kaysi, R. O.; Ahn, T. S.; Müller, A. M.; Bardeen, C. J. The photophysical properties of chromophores at high (100 mM and above) concentrations in polymers and as neat solids. *Phys. Chem. Chem. Phys.* **2006**, *8*, 3453–3459.

(35) Baumann, J.; Fayer, M. D. Excitation transfer in disordered two-dimensional and anisotropic three-dimensional systems: effects of spatial geometry on time-resolved observables. *J. Chem. Phys.* **1986**, *85*, 4087–4107.

(36) Ahn, T. S.; Al-Kaysi, R. O.; Müller, A. M.; Wentz, K. M.; Bardeen, C. J. Self-absorption corrections for solid-state photoluminescence quantum yields obtained from integrating sphere measurements. *Rev. Sci. Instrum.* **2007**, *78*, 086105/1–086105/3.

(37) Baldo, M. A.; Soos, Z. G.; Forrest, S. R. Local order in amorphous organic molecular thin films. *Chem. Phys. Lett.* **2001**, *347*, 297–303.

(38) Gochanour, C. R.; Fayer, M. D. Electronic excited-state transport in random systems. Time-resolved fluorescence depolarization measurements. *J. Phys. Chem.* **1981**, *85*, 1989–1994.

(39) Flors, C.; Oesterling, I.; Schnitzler, T.; Fron, E.; Schweitzer, G.; Sliwa, M.; Herrmann, A.; Auweraer, M. v. d.; Schryver, F. C. D.; Müllen, K.; Hofkens, J. Energy and electron transfer in ethynylene bridged perylene diimide multichromophores. *J. Phys. Chem. C* **2007**, *111*, 4861–4870.

(40) Schlosser, M.; Lochbrunner, S. Exciton migration by ultrafast Förster transfer in highly doped matrices. *J. Phys. Chem. B* **2006**, *110*, 6001–6009.

(41) Yang, J.; Roller, R. S.; Winnik, M. A. Energy migration study of random immobile anthracene derivatives by time-resolved fluorescence anisotropy decays. *J. Phys. Chem. B* **2006**, *110*, 11739–11745.

(42) Laperrière, S. C.; Müllens, J. W.; L'Espérance, D.; Chronister, E. L. Optical energy transfer and trapping in 9-aminoacridine doped sol-gel glasses. *Chem. Phys. Lett.* **1995**, *243*, 114–124.

(43) Powell, R. C.; Soos, Z. G. Singlet exciton energy transfer in organic solids. *J. Lumin.* **1975**, *11*, 1–45.

(44) Gösele, U.; Hauser, M.; Klein, U. K. A.; Frey, R. Diffusion and long-range energy transfer. *Chem. Phys. Lett.* **1975**, *34*, 519–522.

(45) Renschler, C. L.; Faulkner, L. R. Design of an antenna system for the collection of singlet excitation energy. Exciton diffusion among concentrated 9,10-diphenylanthracene centers in polystyrene. *J. Am. Chem. Soc.* **1982**, *104*, 3315–3320.

(46) Joshi, H. C.; Mishra, H.; Tripathi, H. B.; Pant, T. C. Role of diffusion in excitation energy transfer: a time-resolved study. *J. Lumin.* **2000**, *90*, 17–25.

(47) Gomez-Jahn, L.; Kasinski, J.; Miller, R. J. D. Spatial properties of electronic excited state energy transport in three-dimensional disordered systems: picosecond transient grating studies. *Chem. Phys. Lett.* **1986**, *125*, 500–506.

(48) Johnson, G. E. Energy migration and transfer in molecularly doped polymers. *Macromolecules* **1980**, *13*, 145–152.

(49) Chandrasekhar, S. Stochastic problems in physics and astronomy. *Rev. Mod. Phys.* **1943**, *15*, 1–89.

(50) Lunt, R. R.; Giebink, N. C.; Belak, A. A.; Benziger, J. B.; Forrest, S. R. Exciton diffusion lengths of organic semiconductor thin films measured by spectrally resolved photoluminescence quenching. *J. Appl. Phys.* **2009**, *105*, 053711/1–053711/7.

(51) Soos, Z. G.; Powell, R. C. Generalized random-walk model for singlet-exciton energy transfer. *Phys. Rev. B* **1972**, *6*, 4035–4046.

(52) Powell, R. C.; Kepler, R. G. Comments on diffusion theory of luminescent emission from a doped organic solid. *Phys. Status Solidi B* **1973**, *55*, K89–K91.

(53) Ali, M. A.; Ahmed, S. A.; Chokhavatia, A. S. Examination of a generalized model for radiationless energy transfer in dyes. Comparison of theory and experiments. *J. Chem. Phys.* **1989**, *91*, 2892–2897.

(54) Kaschke, M.; Vogler, K. Picosecond study of energy transfer. Deviations from Förster theory—evidence for an inhomogeneous spatial distribution of molecules. *Chem. Phys.* **1986**, *102*, 229–240.

(55) Wang, Z.; Holden, D. A.; McCourt, F. R. W. Monte Carlo simulation of singlet energy migration and trapping in nonrandom chromophore distributions generated by photoraction in glassy polymer matrices. *Macromolecules* **1991**, *24*, 893–900.

(56) Barbosa-García, O.; Struck, C. W. Monte Carlo treatment of the nonradiative energy transfer process for nonrandom placements of dopants in solids. *J. Chem. Phys.* **1994**, *100*, 4554–4568.

(57) Kalogeras, I. M.; Neagu, E. R.; Vassilikou-Dova, A. Free-space and intermolecular interaction effects on the local-chain rotational relaxation dynamics in dye + polymer lasing materials. *Macromolecules* **2004**, *37*, 1042–1053.

(58) Kalogeras, I. M.; Pallikari, F.; Vassilikou-Dova, A. The diverse effect of antiplasticizer in the molecular dynamics of an organic dye-doped polymer observed at different motional lengthscales. *Eur. Polym. J.* **2009**, *45*, 1377–1384.

(59) Beenken, W. J. D.; Pullerits, T. Excitonic coupling in polythiophenes: comparison of different calculation methods. *J. Chem. Phys.* **2004**, *120*, 2490–2495.

(60) Krueger, B. P.; Scholes, G. D.; Fleming, G. R. Calculation of couplings and energy-transfer pathways between the pigments of LH2 by the ab initio transition density cube method. *J. Phys. Chem. B* **1998**, *102*, 5378–5386.

(61) Grage, M. M.-L.; Wood, P. W.; Ruseckas, A.; Pullerits, T.; Mitchell, W.; Burn, P. L.; Sundström, V. Conformational disorder and energy migration in MEH-PPV with partially broken conjugation. *J. Chem. Phys.* **2003**, *118*, 7644–7650.

(62) Scholes, G. D. Long-range resonance energy transfer in molecular systems. *Annu. Rev. Phys. Chem.* **2003**, *54*, 57–87.

(63) Ortiz, W.; Krueger, B. P.; Kleiman, V. D.; Krause, J. L.; Roitberg, A. E. Energy transfer in the nanostar: the role of coulombic coupling and dynamics. *J. Phys. Chem. B* **2005**, *109*, 11512–11519.

(64) Wong, K. F.; Bagchi, B.; Rossky, P. J. Distance and orientational dependence of excitation transfer rates in conjugated systems: beyond the Förster theory. *J. Phys. Chem. A* **2004**, *108*, 5752–5763.

(65) Curutchet, C.; Mennucci, B.; Scholes, G. D.; Beljonne, D. Does Förster predict the rate of electronic energy transfer for a model dyad at low temperature? *J. Phys. Chem. B* **2008**, *112*, 3759–3766.

(66) Rangelowa-Jankowska, S.; Kulak, L.; Bojarski, P. Nonradiative long range energy transfer in donor-acceptor systems with excluded volume. *Chem. Phys. Lett.* **2008**, *460*, 306–310.

(67) Riehl, J. P. Orientation effects in radiationless energy transfer by computer simulation. *J. Phys. Chem.* **1985**, *89*, 3203–3206.

(68) Engström, S.; Lindberg, M.; Johansson, L. B.-A. Monte Carlo simulations of electronic energy transfer in three-dimensional systems: a comparison with analytical theories. *J. Chem. Phys.* **1988**, *89*, 204–213.

(69) Bojarski, P.; Kulak, L.; Bojarski, C.; Kawski, A. Nonradiative excitation transport in one-component disordered systems. *J. Fluoresc.* **1995**, *5*, 307–319.

(70) Bojarski, P.; Kulak, L. Forward and reverse excitation energy transport in concentrated two-component systems. *Chem. Phys.* **1997**, *220*, 323–336.

(71) Kulak, L. Hybrid Monte-Carlo simulations of fluorescence anisotropy decay in disordered two-component systems in the presence of forward and back energy transfer. *Chem. Phys. Lett.* **2008**, *457*, 259–262.

(72) Krystkowiak, E.; Maciejewski, A. Examination of the Smoluchowski-Collins-Kimball model in fluorescence quenching of S2-xanthione. *J. Chem. Phys.* **2002**, *117*, 5802–5809.

(73) Yokota, M.; Tanimoto, O. Effects of diffusion on energy transfer by resonance. *J. Phys. Soc. Jpn.* **1967**, *22*, 779–784.

(74) Birks, J. B. *Photophysics of aromatic molecules; 1 ed.*; J. Wiley & Sons: London, 1970.

(75) Faulkner, L. R. Effects of diffusion on resonance energy transfer. Comparisons of theory and experiment. *Chem. Phys. Lett.* **1976**, *43*, 552–556.

(76) Auerbach, R.; Robinson, G. W.; Zwanzig, R. W. Diffusion modulated donor-acceptor energy transfer in a disordered system. *J. Chem. Phys.* **1980**, 3528–3538.

(77) Stein, A. D.; Peterson, K. A.; Fayer, M. D. Dispersive electronic excitation transport in polymeric solids at and near room temperature. *Chem. Phys. Lett.* **1989**, *161*, 16–22.

(78) Stein, A. D.; Peterson, K. A.; Fayer, M. D. Dispersive excitation transport at elevated temperatures (50−298 K): Experiments and theory. *J. Chem. Phys.* **1990**, *92*, 5622–5635.

(79) Mollay, B.; Lemmer, U.; Kersting, R.; Mahrt, R. F.; Kurz, H.; Kauffmann, H. F.; Bässler, H. Dynamics of singlet excitons in conjugated polymers: Poly(phenylenevinylene) and poly(phenylphenylvinylene). *Phys. Rev. B* **1994**, *50*, 10769–10779.

(80) Meskers, S. C. J.; Hübner, J.; Oestreich, M.; Bässler, H. Dispersive relaxation dynamics of photoexcitations in a polyfluorene film involving energy transfer: experiment and Monte Carlo simulations. *J. Phys. Chem. B* **2001**, *105*, 9139–9149.

(81) Arkhipov, V. I.; Emelianova, E. V.; Bässler, H. On the role of spectral diffusion of excitons in sensitized photoconduction in conjugated polymers. *Chem. Phys. Lett.* **2004**, *383*, 166–170.

(82) Gaab, K. M.; Bardeen, C. J. Anomalous exciton diffusion in the conjugated polymer MEH-PPV measured using a three-pulse pump-dump-probe anisotropy experiment. *J. Phys. Chem. A* **2004**, *108*, 10801–10806.

(83) Madigan, C.; Bulović, V. Modeling of exciton diffusion in amorphous organic thin films. *Phys. Rev. Lett.* **2006**, *96*, 046404/1–046404/4.

(84) Katsuura, K. Exciton migration in one-dimensional molecular random lattices. *J. Chem. Phys.* **1964**, *40*, 3527–3530.

(85) Schönherr, G.; Eiermann, R.; Bässler, H.; Silver, M. Dispersive exciton transport in a hopping system with guassian energy distribution. *Chem. Phys.* **1980**, *52*, 287–298.

(86) Ahn, T. S.; Wright, N.; Bardeen, C. J. The effects of orientational and energetic disorder on Förster energy migration along a one-dimensional lattice, *Chem. Phys. Lett.* **2007**, *446*, 43–48.

(87) Yang, F.; Forrest, S. R. Photocurrent generation in nanostructured organic solar cells. *ACS Nano* **2008**, *2*, 1022–1032.

(88) Athansopoulos, S.; Hennebicq, E.; Beljonne, D.; Walker, A. B. Trap limited exciton transport in conjugated polymers. *J. Phys. Chem. C* **2008**, *112*, 11532–11538.

(89) Walker, A. B. Multiscale modeling of charge and energy transport in organic light-emitting diodes and photovoltaics. *Proc. IEEE* **2009**, *97*, 1587–1596.

(90) Pfister, G.; Scher, H. Dispersive (non-Gaussian) transient transport in disordered solids. *Adv. Phys.* **1978**, *27*, 747–798.

(91) Blumen, A.; Manz, J. On the concentration and time-dependence of the energy transfer to randomly distributed acceptors. *J. Chem. Phys.* **1979**, *71*, 4694–4702.

(92) Klafter, J.; Silbey, R. On electronic energy transfer in disordered systems. *J. Chem. Phys.* **1980**, *72*, 843–852.

(93) Godzik, K.; Jortner, J. Electronic energy transport in substitutionally disordered molecular crystals. *J. Chem. Phys.* **1980**, *72*, 4471–4486.

(94) Huber, D. L.; Hamilton, D. S.; Barnett, B. Time-dependent effects in fluorescent line narrowing. *Phys. Rev. B* **1977**, *16*, 4642–4650.

(95) Huber, D. L. Donor fluorescence at high trap concentration. *Phys. Rev. B* **1979**, *20*, 5333–5338.

(96) Huber, D. L. Fluorescence in the presence of traps. *Phys. Rev. B* **1979**, *20*, 2307–2314.

(97) Fedorenko, S. G.; Burshtein, A. I. What are the GAF and LAF approaches in essence? *Chem. Phys.* **1985**, *98*, 341–349.

(98) Movaghar, B.; Grünewald, M.; Ries, B.; Bässler, H.; Würtz, D. Diffusion and relaxation of energy in disordered organic and inorganic materials. *Phys. Rev. B* **1986**, *33*, 5545–5554.

(99) Sienicki, K.; Mattice, W. L. Forward and reverse energy transfer in the presence of energy migration and correlations. *J. Chem. Phys.* **1989**, *90*, 6187–6192.

(100) Miller, R. J. D.; Pierre, M.; Fayer, M. D. Electronic excited state transport and trapping in disordered systems: picosecond fluorescence mixing, transient grating, and probe pulse experiments. *J. Chem. Phys.* **1983**, *78*, 5138–5146.

(101) Pandey, K. K. Electronic excitation transport, diffusion and trapping. *Chem. Phys.* **1992**, *165*, 123–134.

(102) Peter, G.; Ries, B.; Bässler, H. Singlet exciton migration in a random organic two-component system containing physical and chemical traps. *Chem. Phys.* **1983**, 289–297.

(103) Pandey, K. K.; Joshi, H. C.; Pant, T. C. Excitation energy migration and transfer in a dye pair in PMMA. *J. Lumin.* **1988**, *42*, 197–203.

(104) Pandey, K. K.; Pant, T. C. Migration modulated donor-acceptor energy transfer in PMMA. *J. Lumin.* **1991**, *47*, 319–325.

(105) Tripathy, U.; Bisht, P. B.; Pandey, K. K. Study of excitation energy migration and transfer in 3,3′-dimethyloxacarbocyanine iodide (DMOCI) and o-(6-diethylamino-3-diethylamino-3H-xanthen-9-yl) benzoic acid (RB) in thin films of polyvinyl alcohol. *Chem. Phys.* **2004**, *299*, 105–112.

(106) Misra, V.; Mishra, H. Effect of polymer microenvironment on excitation energy migration and transfer. *J. Phys. Chem. B* **2008**, *112*, 4213–4222.

(107) Narasimhan, L. R.; Bai, Y. S.; Dugan, M. A.; Fayer, M. D. Observation of fast time scale spectral diffusion in a low temperature glass: comparison of picosecond photon and stimulated echoes. *Chem. Phys. Lett.* **1991**, *176*, 335–342.

(108) Baer, B. J.; Crowell, R. A.; Chronister, E. L. High-pressure low-temperature optical dephasing of Rhodamine 101 in PMMA. *Chem. Phys. Lett.* **1995**, *237*, 380–386.

(109) Bardeen, C. J.; Cerullo, G.; Shank, C. V. Temperature-dependent electronic dephasing of molecules in polymers in the range 30 to 300 K. *Chem. Phys. Lett.* **1997**, *280*, 127–133.

(110) Nagasawa, Y.; Yu, J. Y.; Fleming, G. R. Solute-solvent interaction dynamics studied by photon echo spectroscopies in polymer glasses. *J. Chem. Phys.* **1998**, *109*, 6175–6183.

(111) Zilker, S. J.; Kador, L.; Friebel, J.; Vainer, Y. G.; Kol'chenko, M. A.; Personov, R. I. Comparison of photon echo, hole burning and single molecule spectroscopy data on low temperature dynamics of organic amorphous solids. *J. Chem. Phys.* **1998**, *109*, 6780–6790.

(112) Nagasawa, Y.; Seike, K.; Muromoto, T.; Okada, T. Two-dimensional analysis of integrated three-pulse photon echo signals of nile blue doped in PMMA. *J. Phys. Chem. A* **2003**, *107*, 2431–2441.

(113) Athansopoulos, S.; Emelianova, E. V.; Walker, A. B.; Beljonne, D. Exciton diffusion in energetically disordered organic materials. *Phys. Rev. B* **2009**, *80*, 195209/1–195209/7.

(114) Poulsen, L.; Jazdzyk, M.; Communal, J. E.; Sancho-García, J. C.; Mura, A.; Bongiovanni, G.; Beljonne, D.; Cornil, J.; Hanack, M.; Egelhaaf, H. J.; Gierschner, J. Three-dimensional energy transport in highly luminescent host-guest crystals: a quantitative experimental and theoretical study. *J. Am. Chem. Soc.* **2007**, *129*, 8585–8593.

JP910277J